Appl. Phys. B 70, 105–109 (2000) / Digital Object Identifier (DOI) 10.1007/s003409900046

Applied Physics B
Lasers
and Optics

Characterization of nonlinear scattering in colloidal suspensions of silica particles

V. Joudrier[1], **P. Bourdon**[1], **F. Hache**[2], **C. Flytzanis**[2]

[1] Centre Technique d'Arcueil DGA/DCE/ 94114 Arcueil, France
(Fax: +33-1/4231-9992, E-mail: joudrier@etca.fr; bourdon@etca.fr)
[2] Laboratoire d'Optique Quantique, Ecole Polytechnique, 91128 Palaiseau cedex, France
(Fax: +33-1/6933-3017, E-mail: hache@leonardo.polytechnique.fr)

Received: 9 December 1998/Revised version: 22 February 1999/Published online: 19 August 1999

Abstract. We present a quantitative characterization of an optical limiting device based on nonlinear light scattering due to a photoinduced refractive index mismatch in colloidal suspensions of silica particles. We analyze the origin of the optical limiting process by direct measurements of the nonlinear scattering at 532 nm with nanosecond laser pulses and we assess the impact of the interface between the particles and the surrounding liquid in the suspensions.

PACS: 42.20; 42.65; 42.70

The optical limitation is an important issue in several instances of technological interest for protection purposes but also for supressing undesirable laser intensity fluctuations and for pulse and beam reshaping. Several schemes have been proposed that invariably exploit a nonlinear regime either in absorption, refraction, or scattering. The choice of the nonlinear material is an important issue, but the problems here are quite different from those encountered in other nonlinear optical processes.

In a recent paper [1], we demonstrated that a medium consisting of two components (a cell containing small silica particles uniformly dispersed in a surrounding liquid) could exhibit a nonlinear scattering effect at high incident fluence. This property is especially attractive for optical limiting applications: at low energy, the medium is rendered homogeneous by a good refractive index matching between the two components, whereas, at high energy, the intense laser light propagating through this medium makes it a heterogeneous scattering medium because of the photoinduced refractive index mismatch between the silica particles and the surrounding medium. Figure 1 shows the optical limiting principle based on this nonlinear scattering effect. Even though the nonlinear scattering was clearly evidenced in [1] and well separated from other possible mechanisms, a precise characterization of this scattering effect has not been performed yet. The purpose of this paper is to present complementary experiments that allow a full description of this effect and a precise determination of the laser-induced index mismatch.

In the next section, two characterization experiments are described: the measurement of the angular distribution of the scattered light generated in the limiting process and an estimation of the total scattered energy. Numerical modelling of these results within the Debye–Rayleigh–Gans model permits an evaluation of the induced phase mismatch. Previous studies by a pump-probe technique indicated that the physical mechanism responsible for the nonlinear scattering was related to photoinduced modifications taking place at the particle/liquid interface rather than with a photoinduced index modification (Kerr effect) in either of the constituents. To

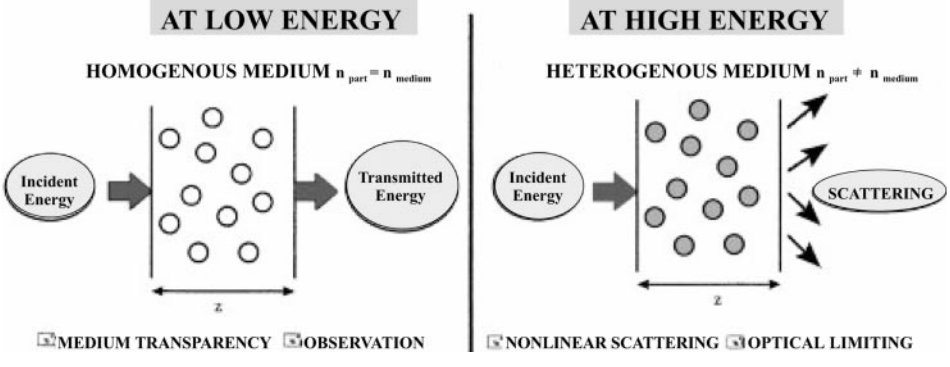

Fig. 1. Limitation principle based on nonlinear light scattering

gain some insight in this problem, we have synthetized a new material with a different interface and studied its optical limitation properties. The results and the comparison of the two samples are given in Sect. 2. From these results, it is possible to get a better understanding of the microscopic phenomena that occur in these materials, as presented in Sect. 4.

1 Characterization of the nonlinear scattering

1.1 Introduction

Let us first recall the main results of [1]. The sample under study was made of small silica particles embedded in a toluene/hexane mixing. Each parameter was chosen with particular attention and controlled during the fabrication process. The silica particles were synthetized with the Stöber method [2] so as to obtain homogeneous spherical particles. These particles were then grafted on their surface with alcohol chains to prevent aggregation and to allow their mixing in a non-polar solvent such as toluene. This solvent was chosen because its refractive index, very close to that of silica, permits us to get easily the index matching between these two components. Precise index matching was obtained by adding hexane in the solution. The final mixing in toluene/hexane was 1/0.8. With this fabrication process, one gets a very uniform distribution of spherical particles. In this first sample, the diameter of the silica particles was $0.11 \pm 0.03\,\mu\text{m}$, the volume fraction and the linear transmission approached 5% and 80%, respectively.

After the sample preparation phase, different experimental investigations were carried out in the nonlinear regime to evidence the presence of nonlinear scattering and optical limitation. We used a frequency-doubled, injection-seeded, Q-switched Nd:YAG laser delivering 10-ns pulses ($\lambda = 532\,\text{nm}$). The first optical tests were made with a classical setup to perform optical limiting and Z-scan experiments with different apertures. From these experiments, it was possible to discriminate among several nonlinear effects such as nonlinear refraction, absorption, and scattering. Finally, the nonlinear scattering was clearly evidenced as the dominant mechanism responsible for the optical limiting behavior of this sample. The dots in Fig. 2 represent a limitation curve obtained with such a sample.

In the following, some complementary experimental investigations are presented to characterize in detail the detected nonlinear scattering, namely its angular distribution of energy and an estimation of the total scattered energy. Theoretical analyses of these investigations allow us to estimate the light-induced index mismatch and corroborate the results of [1].

1.2 Angular distribution of scattered light

The experimental setup used to study the angular distribution of scattered light is a classical one as depicted in the work of K. Nashold et al. [3]. We use the same optical testbed as in [1], except for the f-number of the first focusing lens (which is now 300-mm focal length lens). We do not use a cylindrical cell because of the strong astigmatism introduced by the curved walls of this cell, and we have kept the same rectangular cell as in [1]. The refraction arising from the flat surfaces and the corners, limited by tilting of the cell, is corrected for during the data acquisition. The scattered energy is measured by a sensitive detector which rotates around the sample, allowing measurement in the forward and backward directions. By changing the incident energy (five different values between 2 and 300 μJ), we are able to observe the onset of nonlinear scattering. Figure 3 presents the ratio of scattered to input energy as a function of angle θ for three values of the incident energy (2, 121, and 300 μJ). A logarithm representation was necessary to make the signal observable, given that the laser energy is still very strong along the optical axis (located here at $\theta = 0°$). On this graph however, it is clear that the detected scattered light increases with incident intensity, showing the presence of nonlinear scattering effects at high energy. The data are relevant only within a small angular area ($20° < \theta < 40°$). For small angles, the influence of the transmitted beam is preponderant, and for large angles, the signal-to-noise ratio becomes too small. Note however that no backscattering has been detected

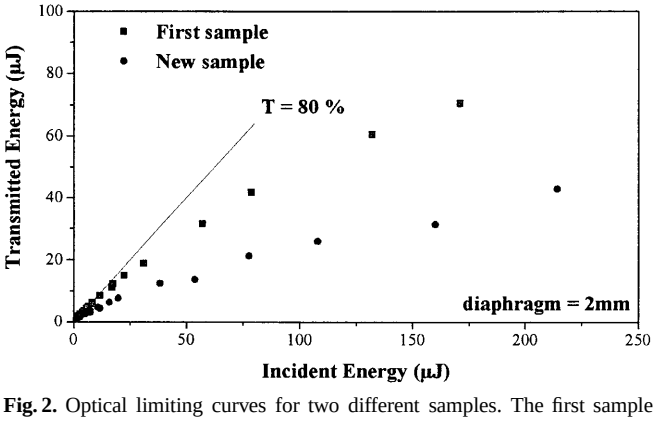

Fig. 2. Optical limiting curves for two different samples. The first sample is made of grafted 0.1-μm-diameter silica particles in a toluene and hexane solution. The second one is constituted of ungrafted 0.1-μm-diameter silica particles in a glycerol and ethylene glycol solution

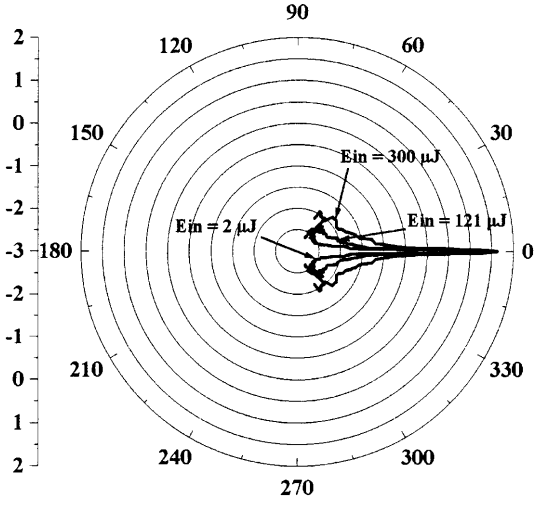

Fig. 3. Logarithmic representation of the ratio of scattered to input energy as a function of angle θ (θ is the angle inside the cell) for three different values of incident energy

in a significant way to be represented on Fig. 3. It is clear that the scattering occurs mainly in the forward direction. It can nevertheless be efficient in an optical limiting device through the use of an appropriate diaphragm.

1.3 Measurement of the scattered energy with an integrating sphere

In the same way, the total scattered energy integrated over all scattering angles can be estimated to complete the characterization of the nonlinear scattering from our sample. To perform this experiment, a 25-cm-diameter integrating sphere was used at the center at which the material was placed. The interior of the sphere was coated with Spectralon, a Lambertian scattering coating with an overall efficiency of 0.99 at $\lambda = 532\,\text{nm}$. The sphere has three ports: two ports through which the laser beam is at first collimated by a 300-mm-focal-length lens into the sample and then exited from the sphere. The last port is used to collect the scattered energy. After complete calibration of this experimental setup and optimization of the focusing lens position to ensure maximum fluence in the sample, a measurement of the total scattered energy is possible, even though the signal-versus-noise ratio is low due to the weak effective efficiency of the integrating sphere (2.3%). The results of this experiment are consistent with the optical limiting curves as can be observed in Fig. 4, where the scattered energy is represented as a function of the incident one. The curve is similar to a (reversed) classical limiting curve and the total scattered energy (38 μJ for an incident energy of 190 μJ) estimated from this experiment is in good agreement with the previous optical limiting experiments.

1.4 Theoretical interpretation

In this section, we want to analyze quantitatively the experimental results presented above. The Debye–Rayleigh–Gans regime was used throughout this theoretical section, as the material parameters fulfill its specific requirement: $ka|m-1| \ll 1$ (k is the wavevector, a the average radius of the spherical particles, m the ratio between the refractive indices of these particles and the surrounding medium). A complete numerical calculation with the Mie formalism has proved to give the same results.

In the Debye–Rayleigh–Gans regime, the scattered intensity can be expressed as a function of the incident one by: $I_\text{s} = NL\Delta\Omega\ \mathrm{d}\sigma_\text{sca}/\mathrm{d}\Omega\ I(*)$. In this equation, N is the particle concentration per volume, L the sample length, $\Delta\Omega$ the solid angle under which the scattered light is measured. $\mathrm{d}\sigma_\text{sca}/\mathrm{d}\Omega$ is the differential scattering cross section, also called the phase function, which can be expressed as: $\mathrm{d}\sigma_\text{sca}/\mathrm{d}\Omega = |X^2|/k^2$ where X is the vector scattering amplitude, perfectly defined for a homogeneous sphere in the simple scattering regime [4]. The parameter X is proportional to the square of the difference in the effective refractive indices of both components and is a function of the parameter ka and of the solid angle $\Delta\Omega$. It is therefore possible to obtain $\mathrm{d}\sigma_\text{sca}/\mathrm{d}\Omega$ from the experiments and, knowing all the material parameters, to calculate the index mismatch Δn for each scattering angle. Equation $(*)$ can also be used to interpret the measurements performed with the integrating sphere, provided one uses its integrated form: $I_\text{s}/I = nL\sigma_\text{sca}$. From the measurement of σ_sca, it is also possible to obtain Δn. For both sets of experiments, the Δn obtained following this procedure depends on the incident intensity, as observed experimentally. Figure 5 shows an example of the Δn variation as a function of the incident energy E_in obtained with the integrating sphere. In this case, as in all the other measurements, we get a linear dependence between Δn and I which we can write: $\Delta n = \Delta n_\text{L} + \Delta n_2 I$. A simple linear regression gives both the linear and nonlinear index differences.

The experimental data displayed in [1] have also been analyzed to evaluate the nonlinearity responsible for the optical limitation. A flux theory of light scattering also based on the Debye–Rayleigh–Gans approximation was used to model the nonlinear propagation in a medium with a spatially random refractive index allowing us to estimate the Δn_L and Δn_2 necessary to explain the observed limitation effect [1].

The values of Δn_L and Δn_2 obtained from the three experiments (optical limitation, distribution of the angular scattering, and integrated scattered energy) are summarized and compared in Table 1. The agreement between the three independent sets of experiments is very good; complementary experiments and their quantitative analysis support thus the previous optical limiting simulation. We can therefore give confidently the values of the index mismatches: $\Delta n_\text{L} \approx 1.4 \times 10^{-2}$ and $\Delta n_2 \approx 1.7 \times 10^{-15}\,\text{m}^2/\text{W}$.

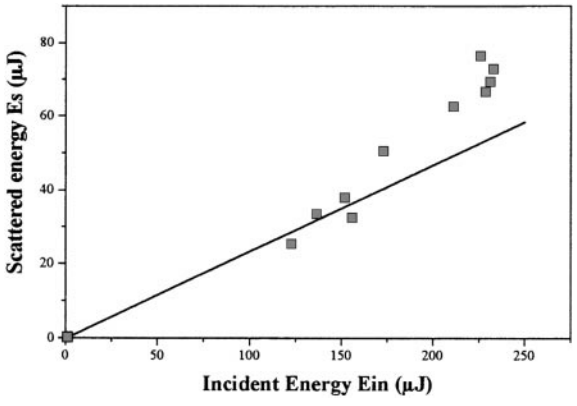

Fig. 4. Representation of the total scattered light measured with the integrating sphere versus the incident energy

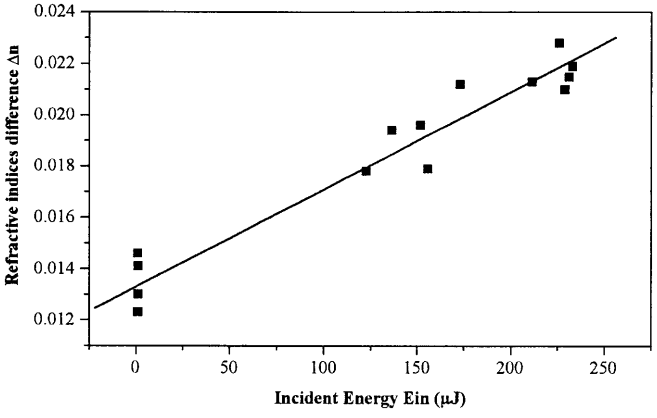

Fig. 5. Representation of the Δn variation as a function of the incident energy E_in

Table 1. Summary of simulation results for Δn_L and Δn_2 from optical limiting, angular scattering, and integrating sphere experiments

Experiments	Δn_L	Δn_2 /m^2/W
limiting curve	1.24×10^{-2}	2.2×10^{-15}
angular scattering	1.54×10^{-2}	1.6×10^{-15}
integrating sphere	1.33×10^{-2}	1.3×10^{-15}

The value obtained for Δn_2 is very strong compared to the bibliographic data for the electronic nonlinearity of silica [5] or those of the surrounding medium [6]. Nonlocal processes such as thermal [6, 7] or electrostrictive [8] ones or whispering gallery modes phenomena [9] can be ruled out after appropriate calculations. Further work seems to be required to assess more precisely the contribution of each parameter of the material to the final effect (such as the solvent, the particles, and the surfactant molecules contribution).

2 New sample and experiments

In order to gain insight into the origin of the strong nonlinearity that exists in our samples, we proceeded to fabricate a new sample in which some of the material parameters are changed. In this new sample, we have chosen to modify the interface between the particles and the surrounding medium by using a solution where no alcohol chains are grafted on the particle surface. However, it is not possible to change only this parameter as these alcohol chains were necessary to maintain the particle in suspension and avoid sedimentation problems. Due to the fact that the silica particles are polar, it is impossible to have the same surrounding medium as in the first sample (toluene and hexane mixing) and a direct transfer of particles without grafted chains in such a medium would induce a rapid particle aggregation, as nothing prevents them from sticking together. One way to avoid this is to use a polar surrounding medium, and we chose a mixing of glycerol and ethylene glycol, on account of their respective polarity, their strong viscosity (maintaining the particles in suspension), and their weak nonlinearities (which are similar to those of toluene and hexane). Furthermore, to permit an easier comparison, the size and the concentration of silica particles are the same as for the previous sample.

This new sample of glycerol, ethylene glycol, and 0.1-μm silica particles in suspension without grafted chains has been tested in the same way as for the first sample. And here again, optical limiting characteristics have been demonstrated, only related to nonlinear scattering. This conclusion is reached after having ruled out all the other possible nonlinear mechanisms (nonlinear absorption or refraction). Moreover, comparing the first sample and the new one, as it is shown in Fig. 2, it is clear that the optical limiting effect is stronger in the second one. The threshold, defined for a decreasing transmission of 20%, is near 1 J/cm^2 for the new material, versus 10 J/cm^2 for the first one. It compares well with the threshold of carbon-black suspension limiters (measured with the same criterion to 0.8 J/cm^2 [10]).

Before discussing the possible origins, it is instructive to study the time response of the optical nonlinearities of the new sample with a dual-beam (pulsed-pump, cw probe) technique. The optical test-bed is described in [1], where it has been used to study the dynamics of the phenomenon in the first sample. The comparison between the fast and slow nonlinear mechanisms of both samples, which can be measured and distinguished by continuous time resolution, allows us to discern the most important parameters. Figure 6 shows an example of typical curves with a millisecond time scale for the first sample and a second time scale for the new one. In both cases, a very strong and fast transmission change is induced by the excitation pulse. However the recorded signals reveal a strong difference in their relaxation times: the decay time is much longer for the new sample (2 s) than for the first one (close to 3 ms).

3 Discussion

Let us first recall that the index mismatch cannot come from the surrounding medium or the silica particles, nor from nonlocal processes as we have shown before [1], and it seems reasonable to attribute the origin of the nonlinear scattering to the particle/solvent interface. This conjecture is also supported by the two pump-probe experiments which show that the mechanism is quite complicated and that many processes with different time scales are involved. Let us examine now the difference between the two samples studied. The nature of the interface between the particles and the solvent is very

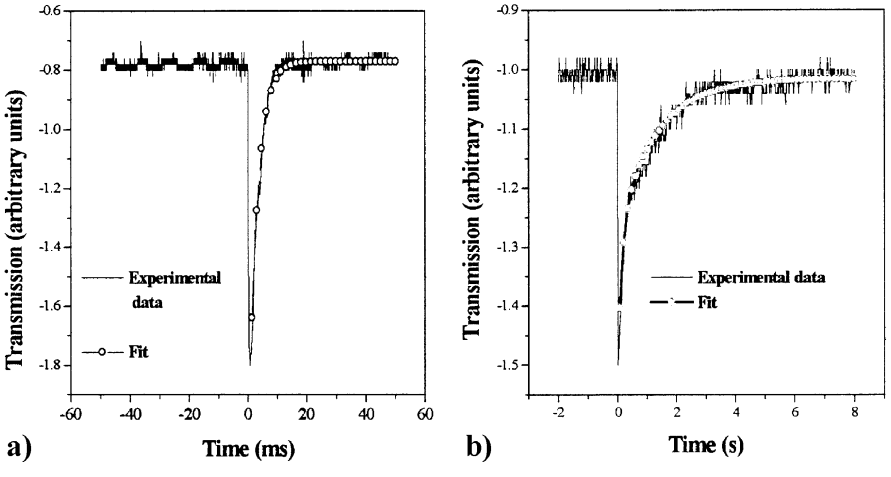

Fig. 6a,b. Transmission time trace after one laser pulse in both samples. A single exponential fit gives a relaxation time around 3 ms for the sample containing the grafted silica particles (**a**), and around 2 s for the other one containing the ungrafted silica particles (**b**)

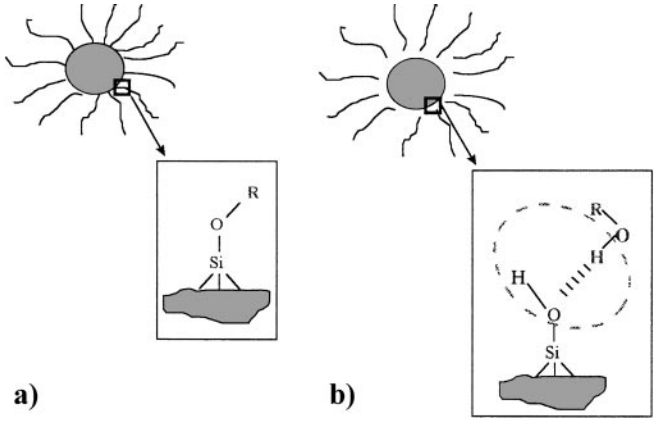

Fig. 7a,b. Microscopic representation of a silica particle when the alcohol chains are grafted with covalent bonds (**a**), or ungrafted with hydrogen bonds (**b**)

different: in the first sample, some alcohol chains are grafted on the particle surface with covalent bonds, whereas in the second material, the solvent polar molecules are connected to the silica particles only by hydrogen bonds. These two kinds of interfaces can certainly explain the difference in the optical limiting behaviors of the two samples, especially in the threshold estimation. Figure 7 shows schematically the particle interfaces in both cases, with an enlarged description of each bond in insert. In the first case, the molecules are more strongly tightened to the surface than in the second one and it is more difficult to perturb the arrangement or to break the bonds, leading to a higher threshold.

The short activation times (not shown in Fig. 6) could therefore be connected in both cases to a photoinduced rearrangement of the molecule layer surrounding the particles which is expected to perturb the pressure locally. This phenomenon could be reversible, assuming that the molecules can get bound again to the particles, or it could be irreversible if there is a photodegradation of the particle surface. In the latter case, the perturbation would last as long as the particles stay in the laser beam. As for the long decay times, the stronger viscosity in the surrounding medium of the new material can certainly explain the slower mechanism in comparison with the previous sample (the viscosity is close to 880 centipoises for the new sample, versus 0.48 for the first one). These long decay times could be connected to the time required by a perturbed particle to get out of the probe beam or come back to its initial equilibrium state through collisions. These times would be proportional to the solvent viscosity, as observed experimentally.

4 Conclusion

In this paper, we have shown that a heterogeneous medium containing spherical silica particles in suspension in a liquid surrounding medium displays nonlinear scattering at high fluence, a property that can be useful for optical limitation purposes. The photoinduced refractive index mismatch has been measured to be very large and cannot be explained by the intrinsic properties of the silica spheres or of the solvent, but originates most probably in the interface between the two constituents. The study of two different samples allows us to confirm this hypothesis and clearly shows that the nature of the surrounding medium (more precisely, its polarity) plays a very important role. The more polar the solvent, the stronger the limitation effect. This feature seems to be connected to the nature (and the strength) of the bonds between the silica particles and the surrounding molecules. Further work should be undertaken to improve this nonlinear scattering effect, for example by increasing the particles concentration to go to the multiple scattering regime. A promising application could be to associate this effect with other optical limiting mechanisms (such as reverse saturable absorption). This could lead to improved behavior of existing devices, especially at high intensity levels.

References

1. V. Joudrier, P. Bourdon, F. Hache, C. Flytzanis: Appl. Phys. B **67**, 627 (1998)
2. W. Stöber, A. Fink: J. Colloid Interface Sci. **26**, 62 (1968)
3. K. Nashold, D.P. Walter: J. Opt. Soc. Am B **12**, 1228 (1995)
4. G.F. Bohren, D.R. Huffman: *Absorption and Scattering of Light by Small Particles* (Wiley, New York 1983) p. 70
5. R. Adair, L.L. Chase, A. Payne: Phys. Rev. B **39**, 3337 (1989)
6. P. Brochard, V. Grolier-Mazza, R. Cabanel: J. Opt. Soc. Am. B **14**, 405 (1997)
7. M. Sheik-Bahae, A.A. Said, T-H. Wei, D.J. Hagan, E.W. Van Stryland: IEEE J. Quantum Electron. **QE-26**, 760 (1990)
8. P.W. Smith, A. Ashkin, W.J. Tomlinson: Opt. Lett. **6**, 284 (1981)
9. H.-B. Lin, A.L. Huston. B.L. Justus, A.L. Campillo: Opt. Lett. **11**, 614 (1986)
10. F. Fougeanet: private communication